Materials Research Bulletin 48 (2013) 823–828

Contents lists available at SciVerse ScienceDirect

Materials Research Bulletin

journal homepage: www.elsevier.com/locate/matresbu

Synthesis of nano-crystalline hydroxyapatite and ammonium sulfate from phosphogypsum waste

Sahar Mousa [a,b,*], Adly Hanna [a]

[a] Inorganic Chemistry Department, National Research Centre, Dokki, P.O.Box:12622, Postal code: 11787 Cairo, Egypt
[b] King Abdulaziz University, Science & Art College, Chemistry Department, Rabigh Campus, P.O. Box:344, Postal code: 21911 Rabigh, Saudi Arabia

ARTICLE INFO

Article history:
Received 13 August 2012
Received in revised form 16 October 2012
Accepted 12 November 2012
Available online 21 November 2012

Keywords:
A. Inorganic compounds
A. Nanostructures
C. X-ray diffraction

ABSTRACT

Phosphogypsum (PG) waste which is derived from phosphoric acid manufacture by using wet method was converted into hydroxyapatite (HAP) and ammonium sulfate. Very simple method was applied by reacting PG with phosphoric acid in alkaline medium with adjusting pH using ammonia solution. The obtained nano-HAP was dried at 80 °C and calcined at 600 °C and 900 °C for 2 h. Both of HAP and ammonium sulfate were characterized by X-ray diffraction (XRD) and infrared spectroscopy (IR) to study the structural evolution. The thermal behavior of nano-HAP was studied; the particle size and morphology were estimated by using transmission electron microscopy (TEM) and scanning electron microscopy (SEM). All the results showed that HAP nano-crystalline and ammonium sulfate can successfully be produced from phosphogypsum waste.

1. Introduction

Phosphogypsum (PG) is an industrial waste derived from phosphoric acid and phosphate fertilizer manufactures by using wet method, where the phosphate ore (flour-apatite mixed with calcium carbonate) is dissolved in phosphoric acid to produce phosphoric acid as filtrate and PG as cake. The amount of the PG waste exceeds considerably than the mass of the product where its amount ranges from 4.5 to 5.5 tons per one ton of P_2O_5 [1]. About 200,000 tons/year of PG are produced in phosphoric acid plants, so it may cause serious storage and environmental problems [2]. In Egypt, hard works were done on the characterization and beneficiation of PG. The complete chemical analysis (Table 1) of PG confirmed that the waste was free from the radioactive elements and heavy metals such as Cd which is the most pollutant element which could hinder the utilization of the waste [3]. Also the waste was applied as adhesive filler and composite material [4]. In the present work, the PG was converted into calcium hydroxyapatite and ammonium sulfate where hydroxyapatite (HAP), $Ca_{10}(PO_4)_6(OH)_2$, is one of the most constituents of the biocompatible inorganic materials used in human hard tissues (bone and teeth) [5,6]. The chemical species constituting HAP crystals (Ca, P, O and H) are expected to have no toxicity [7]. Synthetic hydroxyapatite is a particularly attractive material, which has received considerable attention over the past two decades for bone and tooth implants because of its chemical similarity to natural bone [8]. It also has an importance in many industrial applications, such as catalysis, ion exchange, and gas sensors [9,10]. Number of methods have been used for HAP synthesis, such as solid state reaction, Co-precipitation, hydrothermal reaction, sol–gel synthesis, microemulsion synthesis and mechanochemical synthesis [11–16]. Ammonium sulfate was prepared where it is used largely as an artificial fertilizer for alkaline soils. It is also used as an agricultural spray adjuvant for water soluble insecticides, herbicides and fungicides. Ammonium sulfate is also used in preparation of other ammonium salts and food additive. In biochemistry its precipitation is a common method for purifying proteins [17]. So, the present work aims to use the phosphogypsum waste for preparing both hydroxyapatite nano-crystalline powder and ammonium sulfate at room temperature. The obtained products were characterized by using X-ray diffraction (XRD), infrared absorption spectra (IR), thermal analysis (TG/DSC), scanning electron microscope (SEM) and transmission electron microscope (TEM).

2. Experimental

2.1. Preparation

A very simple method was used for preparation of both hydroxyapatite (HAP) and ammonium sulfate. The starting materials were the phosphogypsum waste (PG), phosphoric acid (85%) and ammonia solution as reactant and agent for pH adjustment. The tap water was used during all steps of preparation.

* Corresponding author. Tel.: +20 233335968; fax: +20 333355192.
E-mail address: dollyriri@yahoo.com (S. Mousa).

0025-5408/$ – see front matter © 2012 Elsevier Ltd. All rights reserved.
http://dx.doi.org/10.1016/j.materresbull.2012.11.067

Table 1
The chemical analysis of phosphogypsum (PG).

Component	%
Insoluble residue	9.50
H_2O	18.5
CaO	29.25
SO^{4-}	41.5
Fe_2O_3	0.10
MgO	0.20
P_2O_5	0.80
F^- (soluble)	0.10
F^- (insoluble)	0.08
Cd	Not detected

Firstly, PG was mixed with tap water with vigorous stirring at room temperature for 30 min. The required amount of phosphoric acid was slowly added dropwise. The pH of the reaction was adjusted to be 11 by adding ammonia solution. The suitable time for complete reaction was determined by repeating the experiment at different time intervals (1.0, 2.0 and 3.0 h). The expected reactions occurred according to the following equation:

$$5CaSO_4{\cdot}2H_2O + 3H_3PO_4 \rightarrow Ca_5(PO_4)_3OH + 5H_2SO_4 + 9H_2O \quad (1)$$

$$10NH_4OH + 5H_2SO_4 \rightarrow 5(NH_4)_2SO_4 + 10H_2O \quad (2)$$

In the next step, the produced HAP has been removed from the solution by filtration and the resulting powder was dried at 80 °C and calcined at 600 °C and 900 °C for 2 h. Also the remainder solution was evaporated to produce the ammonium sulfate material.

2.2. Characterization

The structure of phosphogypsum waste and the phases of all produced samples were investigated by X-ray diffraction (XRD), where the diffraction patterns were obtained by using Bruker D8 advanced X-ray diffractometer with copper (Kα) radiation. For only HAP, the Ca/P ratio was determined by EDX analysis (INCAX-Sight, Oxford Instrument, England.). Infrared (IR) measurement of HAP before and after heat treatment and ammonium sulfate were recorded by (JASCO–FTIR-3000E) infrared spectrometer in range from 4000 to 400 cm^{-1}; the thermal analysis of dried HAP was performed by USA Perkin-Elmer thermogravimetric up to 1000 °C with heating rate 10 °C/min. The micrographs of HAP dried at 80 °C and calcined at 900 °C were taken by scanning electron microscope (SEM: Jeol-JAX–840 A, Japan) with electronic probe microanalyzer and the morphology and particle size were examined by transmission electron microscope (TEM) Jeol JEM-1230 and carried out at 100 keV.

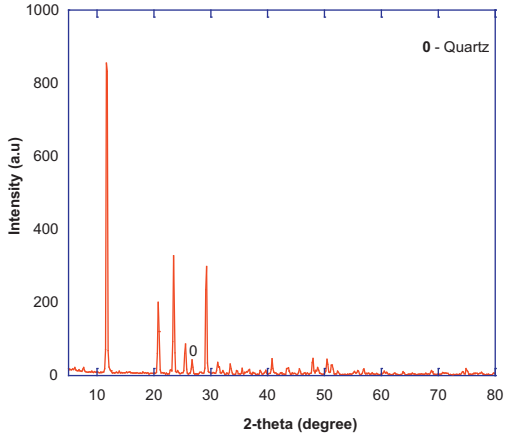

Fig. 1. XRD pattern of phosphogypsum waste ($CaSO_4{\cdot}2H_2O$).

3. Results and discussion

Fig. 1 shows XRD pattern of PG waste, where only one phase of pure gypsum $CaSO_4{\cdot}2H_2O$ [JCPDS (06-0047)] was observed. Also the characteristic peak of quartz (SiO_2) was appearing at *d*-spacing value 3.34 Å with low intensity [JCPDS (01-0649)]. XRD patterns of dried HAP sample and calcined samples at 600 °C and 900 °C are shown in Fig. 2. For dried HAP and calcined sample at 600 °C, XRD patterns indicate a poor crystalline nature of HAP with broad diffraction peaks obtained without any extraneous phases. This means that, pure and homogenous hydroxyapatite could be produced. Calcination temperature plays an important role on the formation of HAP. As the calcination temperature increased from 600 to 900 °C, several peaks of hydroxyapatite become more distinct and narrow which suggested an increase in the degree of crystallinity. Additional crystalline tricalcium phosphate (β-TCP) phase can be observed for the calcined sample at 900 °C. So, XRD results indicated that HAP could be partially decomposed into (β-TCP) as the calcination temperature increased to 900 °C. All the XRD patterns of HAP have the characteristic peak of quartz due to presence of quartz in the starting material (PG). The intensity of

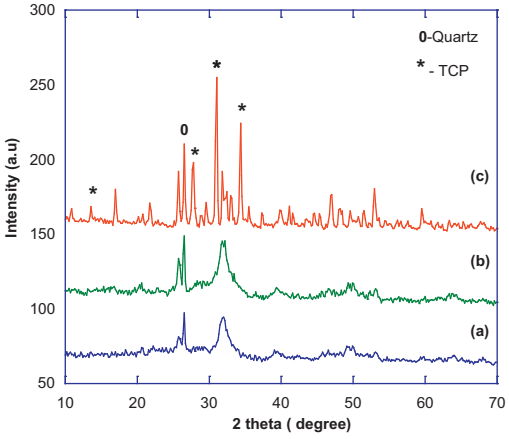

Fig. 2. XRD patterns of dried HAP at 80 °C (a), calcined sample at 600 °C (b) and 900 °C (c).

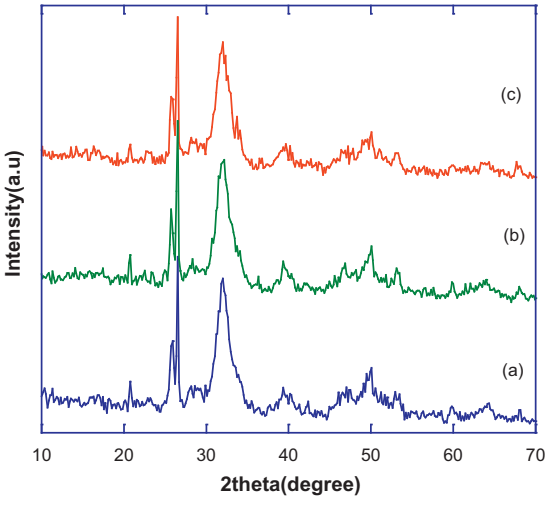

Fig. 3. XRD patterns of as-prepared HAP for 1 h (a), 2 h (b) and 3 h (c) at room temperature.

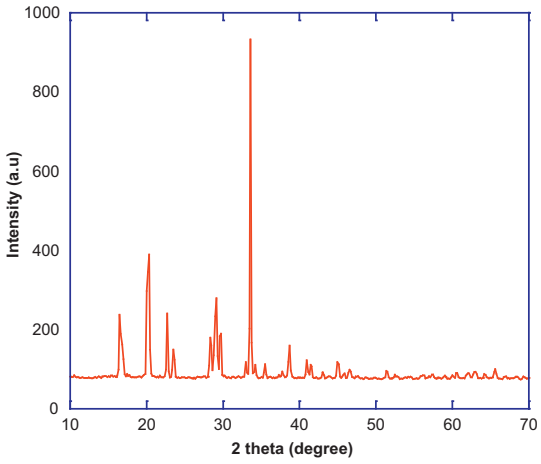

Fig. 4. XRD pattern of as-prepared ammonium sulfate.

quartz peaks occurred sharply at XRD patterns of dried HAP and calcined sample at 600 °C due to the poor crystallinity of HAP but its intensity decreased at XRD pattern of calcined HAP sample at 900 °C due to the good crystallinity of β-TCP. The decomposition of HAP partly into β-TCP was also reported by Raynaud et al. [18].

The suitable time for complete reaction is estimated from XRD patterns as shown in Fig. 3. The patterns show that the reaction is completed after 1 h and an excess of time has no effect on the reaction. So the applied method for HAP preparation does not need long time. This may be another advantage in this work where the reaction occurred at room temperature within short time (1 h).

The XRD pattern of prepared ammonium sulfate sample is shown in Fig. 4. The identification of the product was carried out by comparing the experimental pattern with JCPDS data where a pure phase of $(NH_4)_2SO_4$ [JCPDS (10-0343)] occurred.

EDX data shows that the Ca/P ratio is approximately 1.50. This obtained value close to the Ca/P ratio (1.67) is found in human bone (Fig. 5 and Table 2). The EDX shows also that the HAP contains a tiny amount of quartz.

Table 2
EDX results for chemical composition of HAP.

Element	wt%	at%
C K	5.80	9.27
O K	60.00	72.15
Si K	0.96	0.66
P K	13.24	8.55
Ca K	20.00	9.50

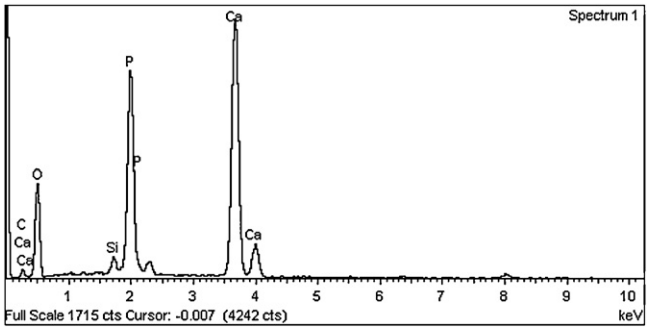

Fig. 5. EDX spectrum of as-prepared HAP.

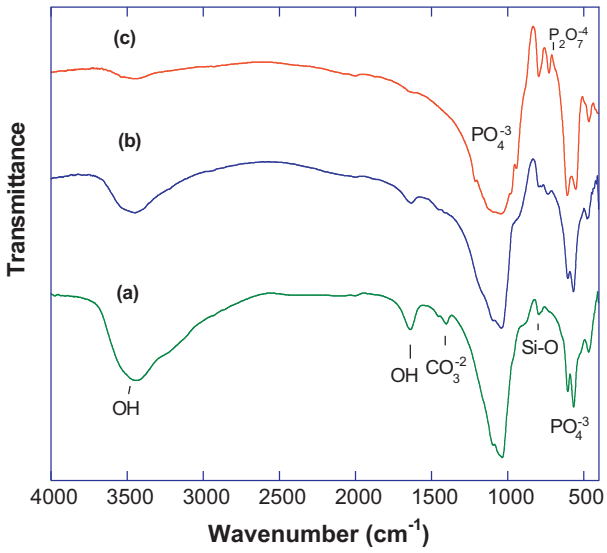

Fig. 6. FTIR spectra of dried HAP at 80 °C (a), calcined sample at 600 °C (b) and at 900 °C (c).

The IR absorption spectra of HAP powders before and after heat treatment at 600 °C and 900 °C are shown in Fig. 6. The characteristic bands of HAP can be observed clearly from the IR spectra. The bands at 1037 cm^{-1} and 1099 cm^{-1} are assigned to ν_3 mode of phosphate group for dried HAP and that calcined at 600 °C [19]. For calcined sample at 900 °C, the transformation of narrow band structures at the same regions into wide absorption bands confirms the formation of β-TCP [20]. For all samples the peak at 470 cm^{-1} was assigned to the ν_2 phosphate mode and the bands at 563 cm^{-1} and 606 cm^{-1} were due to ν_4 phosphate mode [21]. The absorption band at 1630 cm^{-1} reflects H_2O bending mode and a broad band at 3440 cm^{-1} indicates the adsorbed water [22,23]. The bands related to presence of water (crystallization and absorbed water) become weaker by calcination process. For only HAP which dried at 80 °C, the presence of spectral band at 1403 cm^{-1} was due to the entrapment of atmospheric carbon dioxide during preparation [24,25] which is completely disappeared by calcination. At all spectra, an absorption band occurred at 796 cm^{-1} related to presence of quartz [26]. Although no β-$Ca_2P_2O_7$ was detected in XRD patterns, an absorption band attributed to $P_2O_7^{4-}$ group at

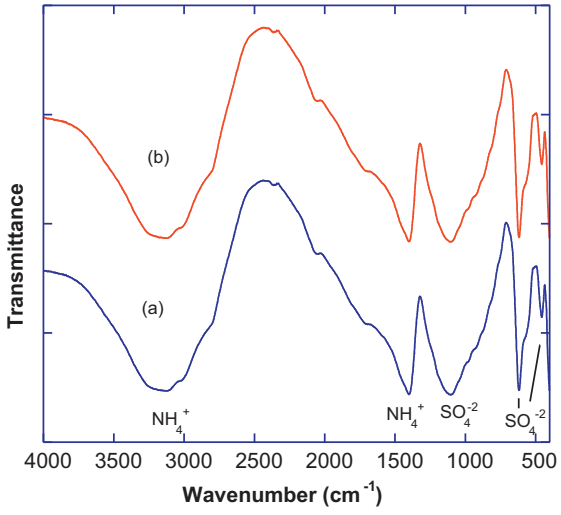

Fig. 7. FTIR spectra of as-prepared ammonium sulfate (a) and the reference (b).

730 cm^{-1} is detected in FTIR analysis after HAP being treated at 600 °C and 900 °C, which suggested the condensation of HPO_4 in Ca-def HAP occurred at temperature < 1000 °C and the formation of β-TCP was supposed to be realized through the calcium pyrophosphate [27]. Both IR and XRD results showed that all HAP samples before and after heat treatment have the apatite structure and the calcined sample at 900 °C has HAP and beta-tricalcium phosphate.

Fig. 7 shows IR spectra of both prepared ammonium sulfate and analytical grade of the same material as reference. The bands at 618 cm^{-1} and 1100 cm^{-1} are assigned to the symmetric deformation and stretch of SO_4^{2-} group. The absorption bands at 1400 cm^{-1} and 3127 cm^{-1} are assigned to the deformation and stretch of NH_4^+ groups. The appearance of absorption band at 458 cm^{-1} is due to vibration of SO_4^{2-} group [28]. The results of IR indicate that the prepared $(NH_4)_2SO_4$ has the same absorption bands as the reference material.

The TG/DSC curves of dried HAP are shown in Fig. 8. Several weight loss steps occurred at TG curve. The first and second steps occurred from room temperature to 400 °C with weight loss of 3.7%, representing the loss of both adsorbed and crystallization water [29].

The third step occurred at 600–775 °C with weight loss of 1.7%, representing the condensation of HPO_4 and formation of $Ca_2P_2O_7$

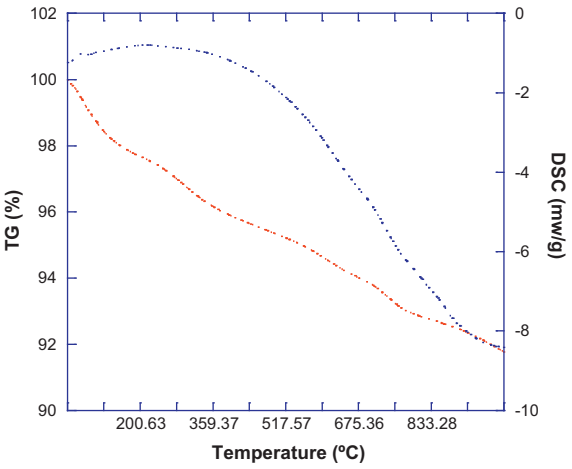

Fig. 8. TG/DSC curves of as-prepared HAP.

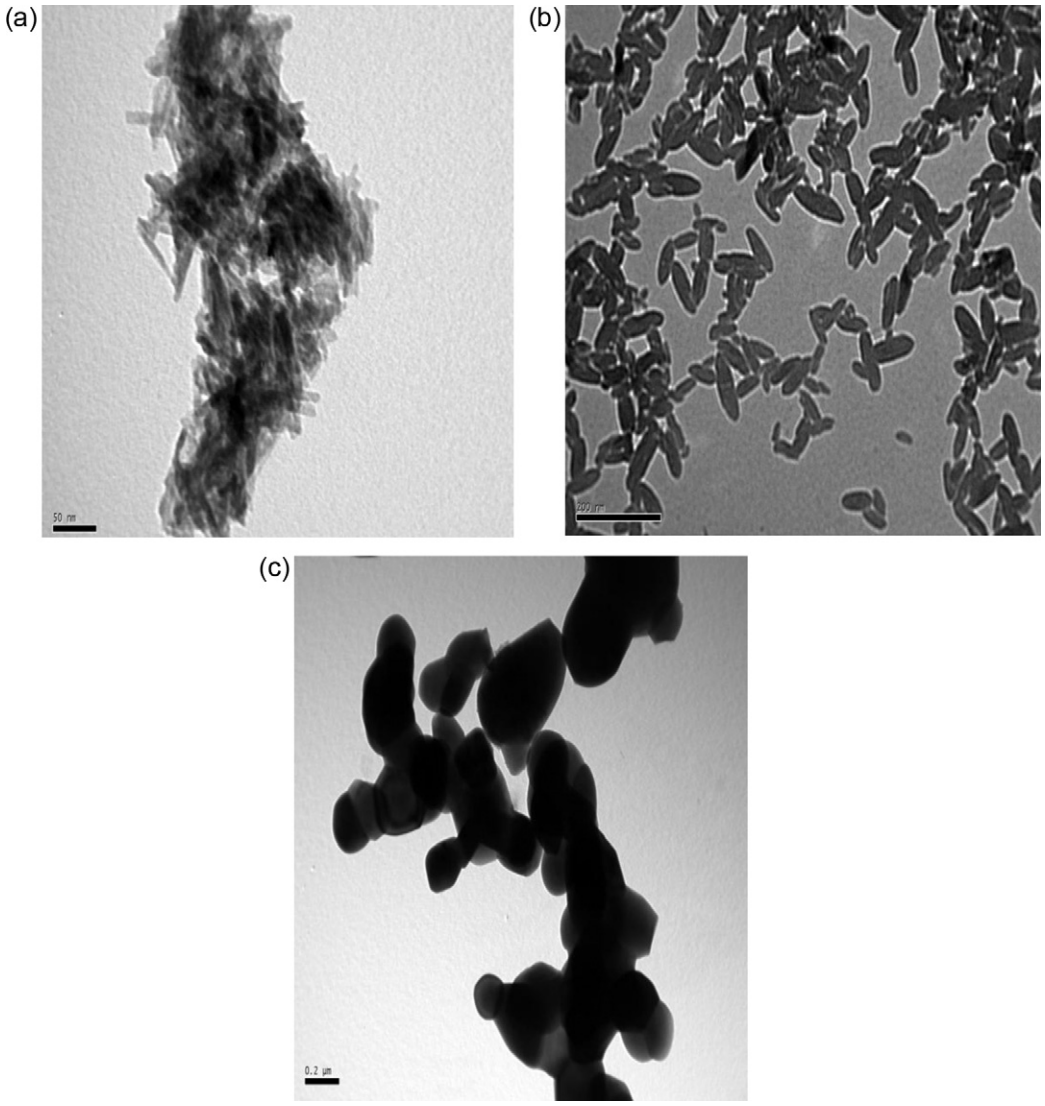

Fig. 9. TEM micrographs of dried HAP at 80 °C (a) and calcined samples at 600 °C (b) and 900 °C (c).

by the following reactions [27,30]:

$$Ca_{10-x}(HPO_4)_x(PO_4)_{6-x}(OH)_{2-x} \rightarrow Ca_{10-x}(P_2O_7)_x(PO_4)_{6-2x}(OH)_{2-x} \quad (3)$$

$$2HPO_4^{2-} \rightarrow P_2O_7^{4-} + H_2O \quad (4)$$

The last step with weight loss of 2.1% occurred at 775–1000 °C, representing a partly conversion of HAP into β-TCP due to dehydroxylation of HAP as the following reaction:

$$Ca_{10-x}(P_2O_7)_x(PO_4)_{6-2x}(OH)_{2-x} \rightarrow 2x(\beta\text{-}Ca_3(PO_4)_2) + (1-x)(Ca_{10}(PO_4)_6(OH)_2) + x(H_2O) \quad (5)$$

The disappearance of sharp endothermic peaks which reflected thermal changes of HAP was also reported by Zhang et al. [30].

TEM micrographs of HAP powders before and after calcination at 600 °C and 900 °C are shown in Fig. 9. The microstructure of both dried HAP and calcined sample at 600 °C are observed to be rod-like particles of 50–57 nm in length and 5–7 nm in width. For calcined sample at 900 °C, the morphology of HAP particles is spherical with an average diameter in the range of 54–74 nm.

Fig. 10 shows the SEM images of dried HAP and calcined samples at 600 °C and 900 °C. For dried HAP and calcined sample at 600°, the samples possess desultory structure and agglomerated particles of a rod-like morphology are formed and also very fine pores are occurred for calcined sample at 600 °C. At 900 °C, the particles become more uniform with an increase in the particle size and also the particles agglomerated in a porous structure [31]. Anee et al. [32] reported that the presence of fine pores may be an advantage for the circulation of physiological fluid when synthetic HAP is used for biomedical purpose.

4. Conclusion

Phosphogypsum (PG) waste was converted into nano-HAP and ammonium sulfate by reacting PG with phosphoric acid in alkaline medium by adding ammonia solution at room temperature for only 1 h. XRD results indicated poor crystalline nature for dried HAP and calcined sample at 600 °C. As the calcination temperature increased to 900 °C, HAP partially decomposed into β-TCP. IR results showed that all HAP samples before and after heat treatments have the apatite's structure. The calcined sample at 900 °C has HAP and β-TCP structures. The thermal analysis showed a partly conversion of HAP into β-TCP due to dehydroxylation of HAP which occurred up to 700 °C. TEM micrographs of dried HAP showed rod-like particles of 50–57 nm in length and 5–7 nm in width. For calcined sample at 900 °C, the HAP has spherical shape with particle size of 54–74 nm. SEM images of dried HAP showed desultory structure and agglomerated particle of rod-like morphology. For calcined sample, an increase in the particle size and

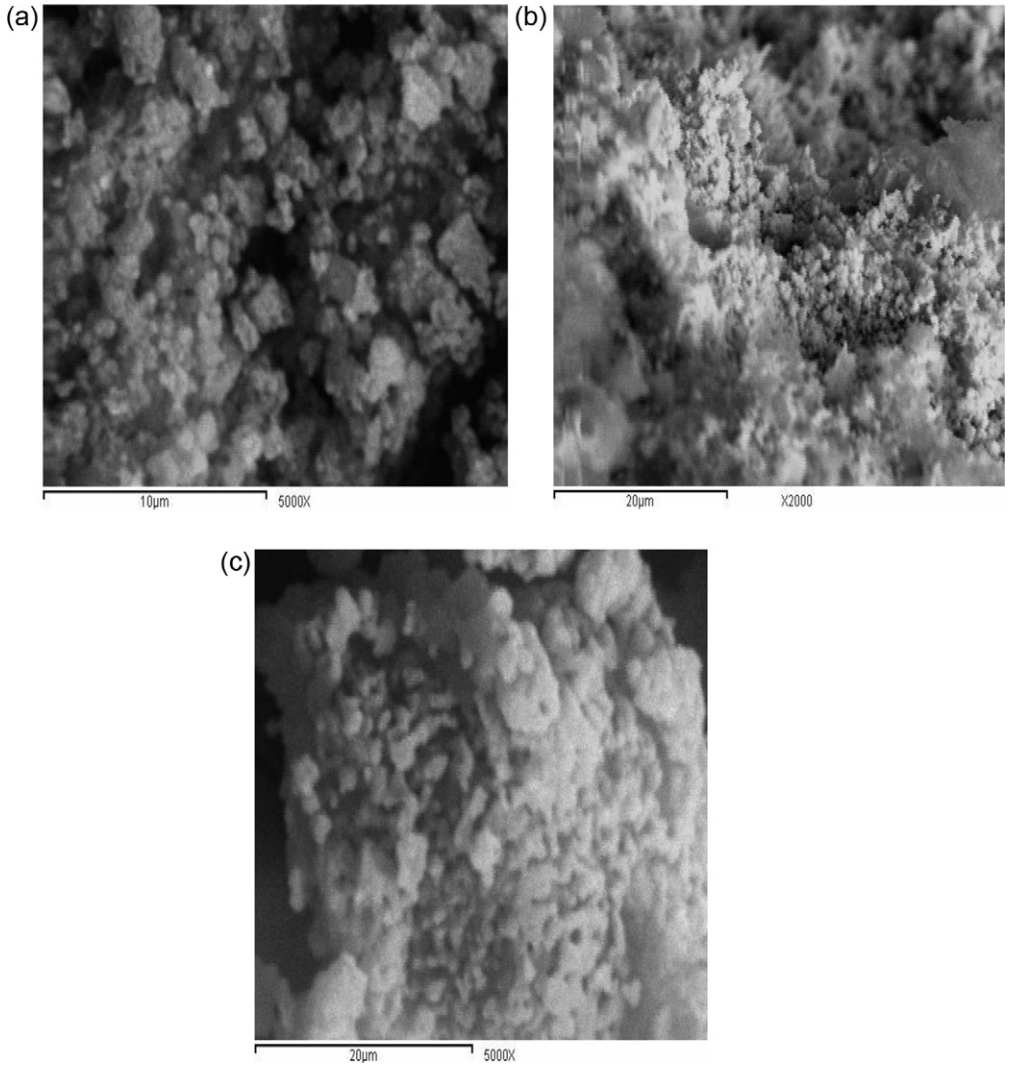

Fig. 10. SEM images of dried HAP at 80 °C (a) and calcined samples at 600 °C (b) and 900 °C (c).

the particles agglomerated in a porous structure. For ammonium sulfate, both XRD and IR results showed the formation of pure phase of $(NH_4)_2SO_4$.

References

[1] H. Tayibi, M. Choura, F.A. Lopez, F.J. Alguacil, A. Lopez-Delgado, J. Environ. Manage. 90 (2009) 2377–2386.
[2] A. Carbonell-Barrachina, R.D. Delaune, A. Jugsujinda, Waste Manage. 22 (2002) 657–665.
[3] A.A. Hanna, A.I.M. Akarish, S.M. Mousa, J. Mater. Sci. Technol. 15 (1999) 431–434.
[4] A.A. Hanna, Y.M. Abu-Ayana, S.M. Mousa, J. Mater. Sci. Technol. 16 (2000) 439–444.
[5] A.N. Hayati, H.R. Rezaie, S.M. Hosseinalipour, Mater. Lett. 65 (2011) 736–739.
[6] Y. Lui, D. Hou, G. Wang, Mater. Chem. Phys. 86 (2004) 69–73.
[7] R. Murugan, S. Ramakrishna, Compos. Sci. Technol. 65 (2005) 2385–2405.
[8] M. Jarcho, C.H. Bolen, M.B. Thomas, J.F. Kay, J. Mater. Sci. 11 (1976) 2027–2035.
[9] J. Batton, A.J. Kadaksham, A. Nzihou, P. Singh, N. Aubry, J. Hazard. Mater. A 139 (2007) 461–466.
[10] A. Mortier, J. Lemaitre, J. Solid State Chem. 78 (1989) 215–219.
[11] J. Tan, M. Chen, J. Xia, Appl. Surf. Sci. 255 (2009) 8774–8779.
[12] I.S. Neira, Y.V. Kolen'ko, O.I. Lebedev, G.V. Tendeloo, H.S. Gupta, F. Guitian, M. Yoshimura, Cryst. Growth 9 (2009) 466–474.
[13] B. Jokic, M. Mitrid, V. Radmilovid, S. Drmanic, R. Petrovic, D. Janackovic, Ceram. Int. 37 (2011) 167–173.
[14] K. Teshima, S.H. Lee, M. Sakurai, Y. Kameno, K. Yubuta, T. Suzuki, T. Shishido, M. Endo, S. Oishi, Cryst. Growth 9 (2009) 2937–2940.
[15] C. Huang, Y.B. Zhou, Z.M. Tang, X. Guo, Z.Y. Qian, S.B. Zhou, Dalton Trans. 40 (2011) 5026–5031.
[16] K. Furuichi, Y. Oaki, H. Imai, Chem. Mater. 18 (2006) 229–234.
[17] J. Arthington, J. Rechcigl, G. Yost, L. MacDowell, M. Fannimg, J. Anim. Sci. 80 (2002) 2507–2512.
[18] S. Raynaud, E. Champion, D. Bernache-Assllant, P. Thomas, Biomaterials 23 (2002) 1065–1072.
[19] K.C. Blakeslee, R.A. Condrate, J. Am. Ceram. Soc. 54 (1971) 559–563.
[20] M.H. Fathi, E.M. Zahrani, J. Cryst. Growth 311 (2009) 1392–1403.
[21] I. Mobasherpour, M. Soulati, A. Kazemzadeh, M. Zakeri, J. Alloys Compd. 430 (2007) 330–333.
[22] M. Kawata, H. Uchida, K. Itatani, I. Okada, S. Koda, M. Aizawa, J. Mater. Sci. Mater. Med. 15 (2004) 817–823.
[23] H.K. Varma, S.S. Babu, Ceram. Int. 31 (2005) 109–114.
[24] T.A. Kuriakose, S.N. Kalkura, M. Palanichamy, D. Arivuoli, K. Dierks, G. Boceli, C. Betzel, J. Cryst. Growth 263 (2004) 517–523.
[25] Z.H. Cheng, A. Yasukawa, K. Kandor, T. Ishikawa, Langmuir 14 (1998) 6681–6686.
[26] J. Hlavay, K. Jonas, S. Elek, J. Inczedy, Clay Clay Miner. 26 (1978) 139–143.
[27] A. Mortier, J. Lemaite, P.G. Rovxhet, Thermochim. Acta 143 (1989) 265–282.
[28] X. Zhu, M. Elomaa, F. Sundholm, C.H. Lochmuller, Polym. Degrad. Stab. 62 (1998) 487–494.
[29] H. Monma, S. Ueno, T. Kanazawa, J. Chem. Technol. Biotechnol. 31 (1981) 15–24.
[30] H. Zhang, M. Zhang, Mater. Chem. Phys. 126 (2011) 642–648.
[31] B. Cengiz, Y. Gokce, N. Yildiz, Z. Aktas, A. Calimli, Physicochem. Eng. Aspects 322 (2008) 29–33.
[32] T.K. Anee, M. Ashok, M. Palanichany, S.N. Kalkura, Mater. Chem. Phys. 80 (2003) 725–730.